European Journal of Radiology Open 10 (2023) 100481

Contents lists available at ScienceDirect

European Journal of Radiology Open

journal homepage: www.elsevier.com/locate/ejro

Simultaneous assessment of heart and lungs with gated high-pitch ultra-low dose chest CT using artificial intelligence-based calcium scoring

Florian Andre [a,b,*], Sebastian Seitz [b], Philipp Fortner [b], Thomas Allmendinger [c], André Sommer [b], Matthias Brado [b], Roman Sokiranski [b], Joana Fink [d], Hans-Ulrich Kauczor [e], Claus P. Heussel [f,h], Felix Herth [g,h], Norbert Frey [a], Johannes Görich [b], Sebastian J. Buss [b]

[a] University of Heidelberg, Department of Cardiology, Angiology and Pneumology, Heidelberg, Germany
[b] MVZ-DRZ Heidelberg, Heidelberg, Germany
[c] Siemens Healthcare, Forchheim, Germany
[d] AstraZeneca, Wedel, Germany
[e] University of Heidelberg, Department of Diagnostic and Interventional Radiology, Heidelberg
[f] University of Heidelberg, Thoraxklinik, Department of Diagnostic and Interventional Radiology with Nuclear Medicine, Heidelberg, Germany
[g] University of Heidelberg, Thoraxklinik, Department of Pneumology and Critical Care Medicine, Heidelberg, Germany
[h] Translational Lung Research Centre Heidelberg, Member of the German Centre for Lung Research (DZL), Heidelberg, Germany

GRAPHICAL ABSTRACT

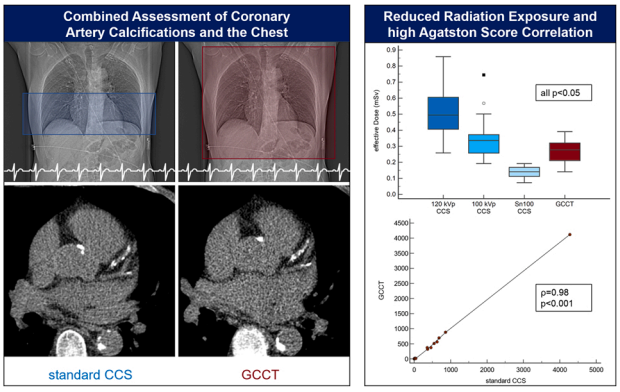

ARTICLE INFO

Keywords:
Coronary artery disease
Coronary artery calcium scoring
Chest CT
Tin-filter
Dose reduction
Artificial intelligence

ABSTRACT

Purpose: The combined testing for coronary artery and pulmonary diseases is of clinical interest as risk factors are shared. In this study, a novel ECG-gated tin-filtered ultra-low dose chest CT protocol (GCCT) for integrated heart and lung acquisition and the applicability of artificial intelligence (AI)-based coronary artery calcium scoring were assessed.

Methods: In a clinical registry of 10481 patients undergoing heart and lung CT, GCCT was applied in 44 patients on a dual-source CT. Coronary calcium scans (CCS) with 120 kVp, 100 kVp, and tin-filtered 100 kVp (Sn100) of controls, matched with regard to age, sex, and body-mass index, were retrieved from the registry (n_{total}=176,

* Correspondence to: University of Heidelberg, Department of Cardiology, Angiology and Pneumology, Im Neuenheimer Feld 410, Heidelberg 69120, Germany.
E-mail address: florian.andre@med.uni-heidelberg.de (F. Andre).

https://doi.org/10.1016/j.ejro.2023.100481
Received 13 October 2022; Received in revised form 10 January 2023; Accepted 9 February 2023

66.5 (59.4–74.0) years, 52 men). Automatic tube current modulation was used in all scans. In 20 patients undergoing GCCT and Sn100 CCS, Agatston scores were measured both semi-automatically by experts and by AI, and classified into six groups (0, <10, <100, <400, <1000, ≥1000).
Results: Effective dose decreased significantly from 120 kVp CCS (0.50 (0.41–0.61) mSv) to 100 kVp CCS (0.34 (0.26–0.37) mSv) to Sn100 CCS (0.14 (0.11–0.17) mSv). GCCT showed higher values (0.28 (0.21–0.32) mSv) than Sn100 CCS but lower than 120 kVp and 100 kVp CCS (all $p < 0.05$) despite greater scan length. Agatston scores correlated strongly between GCCT and Sn100 CCS in semi-automatic and AI-based measurements (both $\rho = 0.98$, $p < 0.001$) resulting in high agreement in Agatston score classification ($\kappa = 0.97$, 95% CI 0.92–1.00; $\kappa = 0.89$, 95% CI 0.79–0.99). Regarding chest findings, further diagnostic steps were recommended in 28 patients.
Conclusions: GCCT allows for reliable coronary artery disease and lung cancer screening with ultra-low radiation exposure. GCCT-derived Agatston score shows excellent agreement with standard CCS, resulting in equivalent risk stratification.

1. Introduction

Cardiovascular and pulmonary diseases belong to the leading causes of morbidity and mortality worldwide, showing an ongoing increase in prevalence in the recent decade [1]. Strategies for their early detection and the risk stratification of patients are of great clinical and socio-economic interest. Computed tomography (CT) of the lungs has been shown to decrease cancer-associated mortality in risk populations [2,3]. It has been recommended by several medical societies and several countries have introduced lung cancer screening programs employing low dose chest CT [4,5]. Cardiovascular and pulmonary diseases such as chronic obstructive pulmonary disease (COPD) and lung cancer share several risk factors such as smoking, unhealthy dietary patterns, air pollution, and age. Consequently, a significant proportion of patients undergoing lung cancer screening CT show coronary artery calcifications and require medical therapy according to established risk stratification models [6–8]. While coronary artery calcification measured by ECG-gated cardiac CT is an established marker for coronary artery disease (CAD) and a robust predictor for adverse events, the assessment of coronary artery calcifications in ungated lung CT shows promising results but is less than ideal as it does not allow for their exact quantification [9].

In recent years, advancements in CT scanner technology including the use of high-pitch acquisitions and tin-filters have enabled the use of ultra-low dose protocols for unenhanced chest CT as well as for coronary calcium scans (CCS) in clinical routine resulting in significant radiation dose savings [10–12]. Hence, the combined assessment of the lungs and coronary calcifications with high diagnostic quality at the cost of very low radiation exposure seems feasible. Recently, an ECG-gated tin-filtered ultra-low dose chest CT protocol (GCCT) was introduced, which combines a tin-filter with an ECG-gated high-pitch spiral acquisition. Furthermore, automatic coronary artery calcium scoring (CACS) using artificial intelligence (AI) has become feasible, which may facilitate and accelerate image analysis. This is the first study assessing the GCCT with regard to clinical applicability, measurement accuracy, radiation dose saving, and applicability of AI-based CACS.

2. Materials and methods

2.1. Study population

Patients undergoing clinically indicated CT examinations of the chest and the heart were enrolled in a clinical registry. Out of 10 481 patients included between November 2014 and July 2021, a subgroup of 44 patients was identified, in whom the novel GCCT was used due to contraindications to or refusal of contrast agent application between June 2020 and June 2021. Data on controls, who had undergone standard CCS with 120 kVp, 100 kVp, or tin-filtered 100 kVp (Sn100), were retrospectively retrieved from the registry. Of note, controls were individually matched to the subjects of the GCCT group with regard to age, sex, and body mass index (BMI). For correlation and agreement analyses, datasets of 20 patients, who had a GCCT scan and a standard Sn100 CCS during the same examination, were obtained from the registry.

The CT examinations were based on clinical indications provided by referring physicians and approval for the retrospective scientific data analysis was obtained from the local ethics committee. The registry study is listed at clinicaltrials.gov (NCT03815123).

2.2. Acquisition protocols

CT examinations were performed on a dual-source CT scanner of the 3rd generation (SOMATOM Force, Siemens Healthcare, Forchheim, Germany). An anterior-posterior topogram was used for the planning of the subsequent CCS or GCCT scan. For standard CCS, the scan length included the heart, whereas the GCCT included the entire chest. The detector configuration was 192 × 0.6 mm and the pitch factor was 3.2. Due to the advancement of CCS protocols in recent years, dedicated CCS with tube potentials of 120 kVp, 100 kVp, or 100 kVp with a tin-filter (Sn100) for spectral shaping were available in the registry, as mentioned above. The GCCT combined a tube potential of 100 kVp with a tin-filter. Automatic tube current modulation (CareDose4D) was applied in all scans.

2.3. Image reconstruction and analysis

Images for CACS were reconstructed with a slice thickness of 3.0 mm and an increment of 1.5 using the dedicated Qr36 kernel for 120 kVp CCS and 100 kVp CCS and the Sa36 kV-independent reconstruction algorithm for Sn100 CCS and GCCT scans. This algorithm enables an artificial 120 kVp equivalent CT image reconstruction, which allows the calculation of an Agatston-equivalent calcium score based on the conventional scoring thresholds, regardless of the tube potential and filter setting of the original CT acquisition [13]. The Agatston score equivalent was measured semi-automatically applying a threshold of 130 HU and using dedicated analysis software (syngo.via, Siemens Healthcare, Forchheim, Germany) by experienced radiologists and cardiologists (each >5 years of experience in cardiac CT). Additionally, observer-independent CACS of the GCCT scans and standard CCS were performed in the subset of patients having undergone both acquisitions using an AI, which had been validated in a previous study [14]. Patients were classified into six groups according to their coronary artery calcifications (0: absent, <10: minimal, <100: mild, <400: moderate, <1000: severe, and ≥1000: extensive) as described before [15]. For the assessment of the chest including the lungs and mediastinum, images were reconstructed with a slice thickness of 3.0 mm and an increment of 1.5 using the Br40 and the Bl57 kernel. Additional reconstructions, e.g., with higher spatial resolution, were performed, if required for diagnostics.

The volumetric computed tomography dose index ($CTDI_{vol}$), the dose length product (DLP), and the exposure time were derived from the dose reports of the scanner. Effective radiation exposure was estimated using a conversion factor of 0.017 mSv/mGy*cm [16].

2.4. Statistics

Continuous data are reported uniformly as median and interquartile range since part of the data showed a non-parametric distribution in the D'Agostino-Pearson test. Categorial data are reported as numbers and proportions. The Kruskal-Wallis test with a post-hoc analysis according to Conover and a Jonckheere-Terpstra trend test were used for the comparison of different groups. Spearman's rho (ρ) was used to assess correlations in non-parametric data. The Chi-squared test was applied for the analysis of categorical data. Agreement in patient classification was assessed using Kappa (κ) with linear weights. A p-value < 0.05 was regarded as statistically significant. Analyses were conducted using dedicated statistical software (MedCalc Statistical Software version 20, MedCalc Software, Ostend, Belgium).

3. Results

The final study population included 176 patients (66.5 (59.4–74.0) years, 52 men, 124 women) consisting of the GCCT (n = 44) and the three matched CCS groups (120 kVp, 100 kVp, Sn100, each n = 44). Age, BMI, and sex distribution did not differ significantly between groups (Table 1, Fig. 1). Arterial hypertension was reported in 105 patients, hyperlipidemia in 89 patients, smoking in 13 patients, diabetes in 24 patients, and family history of CAD in 91 patients.

The $CTDI_{vol}$ differed significantly between all CCS groups with 120 kVp CCS (1.6 (1.3–1.9) mGy) showing the highest value, followed by 100 kVp CCS (1.1 (0.8–1.2) mGy) and Sn100 CCS (0.5 (0.4–0.6) mGy; overall $p < 0.001$, $p < 0.05$ for post-hoc group comparisons). GCCT showed a significantly lower $CTDI_{vol}$ (0.5 (0.4–0.5) mGy) than 120 kVp CCS and 100 kVp CCS, whereby the difference to Sn100 CCS was not significant due to the similar tube settings. The DLP decreased significantly from 120 kVp CCS (29.1 (23.9–35.6) mGy*cm) to 100 kVp CCS (19.8 (15.2–21.0) mGy*cm) to Sn100 CCS (8.3 (6.6–9.9) mGy*cm; overall $p < 0.001$, $p < 0.05$ for post-hoc group comparisons). DLP in the GCCT group (16.3 (12.4–18.9) mGy*cm) was significantly higher than in the Sn100 CCS group due to the greater scan length, but significantly lower than in the 120 kVp CCS and the 100 kVp CCS group. There was a decrease in the estimated effective dose from the 120 kVp CCS group (0.50 (0.41–0.61) mSv) to the 100 kVp CCS group (0.34 (0.26–0.37) mSv) to the Sn100 CCS group (0.14 (0.11–0.17) mSv). The estimated effective dose in the GCCT group (0.28 (0.21–0.32) mSv) was lower than in the 120 kVp CCS and the 100 kVp CCS group but higher than in the Sn100 CCS group. All differences were statistically significant (overall $p < 0.001$, $p < 0.05$ for post-hoc group comparisons). Data are displayed in Fig. 2.

An expert-based analysis showed a strong and highly significant correlation between Agatston score equivalents derived from GCCT scans and standard Sn100 CCS ($\rho = 0.98$, $p < 0.001$). Accordingly, the classification of coronary calcifications showed a high agreement between the GCCT scans and standard Sn100 CCS ($\kappa = 0.97$, 95% CI 0.92–1.00) using six different classes as described above. Only one case was classified differently (severe in the Sn100 CCS and moderate in the GCCT scan). Using solely the AI for observer-independent CACS, the correlation between GCCT scans and standard Sn100 CCS was strong and highly significant ($\rho = 0.98$, $p < 0.001$) and subsequent case classification showed a good agreement ($\kappa = 0.89$, 95% CI 0.79–0.99). The data are displayed in Fig. 3 and an image sample is given in Fig. 4.

Main pulmonary findings were emphysema in 28 patients, lung or pleural nodules (with or without suspected malignancy) in 26 patients, other pulmonary pathologies (e.g., fibrosis, infiltrates) in 48 patients, and pleural lesions in 49 patients. Further diagnostic testing or follow-up examinations were recommended in 28 patients (15.9%).

The exposure time of the GCCT scan was 0.55 (0.51–0.58) s. The image quality of the dedicated chest reconstructions was good and allowed for diagnostic assessment in all cases. The estimated radiation dose derived from 10 481 CCS drawn from the registry declined significantly over time ($p < 0.05$) as displayed in Fig. 5.

4. Discussion

4.1. Rationale of combined heart and lung assessment

The recently introduced GCCT allows for a reliable assessment of the lungs and coronary artery calcifications for CAD risk stratification with low radiation exposure in clinical routine.

Since risk factors for cardiovascular and pulmonary diseases show considerable overlap, a combined screening approach seems reasonable in risk populations, estimated to be 7 000 000 in the USA alone [17]. Coronary artery calcification is the most predictive cardiovascular risk factor improving risk stratification even in patients eligible for lung cancer screening [7,8,18–20]. Reporting coronary artery calcifications in all non-contrast chest examinations is therefore recommended [21]. In addition, coronary artery calcification is an independent risk factor for cancers, especially lung cancer as shown in a recent analysis of the MESA study underlining its potential role for combined risk evaluation [22]. Although several studies showed a reasonable agreement between coronary calcium estimations in non-gated chest CT examinations and dedicated CCS, such approaches are not optimal [9]. They are associated with higher inter-observer and inter-scan variabilities and showed an underestimation of severe coronary calcifications in 19% and false-negative results in 9% of subjects in a meta-analysis [23–25]. As the exclusion of coronary artery calcification, the so-called "Power of Zero", is a strong negative predictor of cardiovascular events and may allow a downward risk classification of patients, the detection of even minimal calcifications is crucial [26]. Thus, the implementation of a gated CCS in chest CT examinations has been proposed [9,17,24,27,28]. Besides the clinical advantages of assessing several major diseases such as CAD, COPD, and lung cancer in a single CT scan, such an approach may be more cost-effective than two separate examinations. Recent advances in image acquisition and post-processing have rendered the creation of ECG-gated ultra-fast ultra-low dose CT protocols possible.

4.2. Application of advanced imaging techniques

In recent years, different dose-saving techniques for CCS have been introduced and their use has resulted in a significant reduction of

Table 1
Demographic parameters of the study population.

	120 kVp CCS	100 kVp CCS	Sn100 CCS	GCCT	p-value
Sex (male)	13 (29.5%)	13 (29.5%)	13 (29.5%)	13 (29.5%)	1.00
Age (years)	67.2 (60.4–75.8)	66.2 (59.3–73.2)	66.5 (60.4–73.7)	66.4 (58.8–72.4)	0.98
BMI (kg/m^2)	27.2 (24.2–29.7)	26.9 (23.8–29.5)	25.8 (23.3–29.9)	26.2 (23.8–30.0)	0.99
Height (cm)	168.0 (163.5–172.0)	167.0 (160.0–174.5)	165.0 (160.5–170.0)	165.5 (160.0–175.0)	0.55

Values are given as numbers and proportions or as medians and interquartile ranges.
BMI: body mass index CCS: coronary calcium scan, GCCT: ECG-gated tin-filtered ultra-low dose chest CT, Sn100: tin-filtered 100 kVp calcium scoring

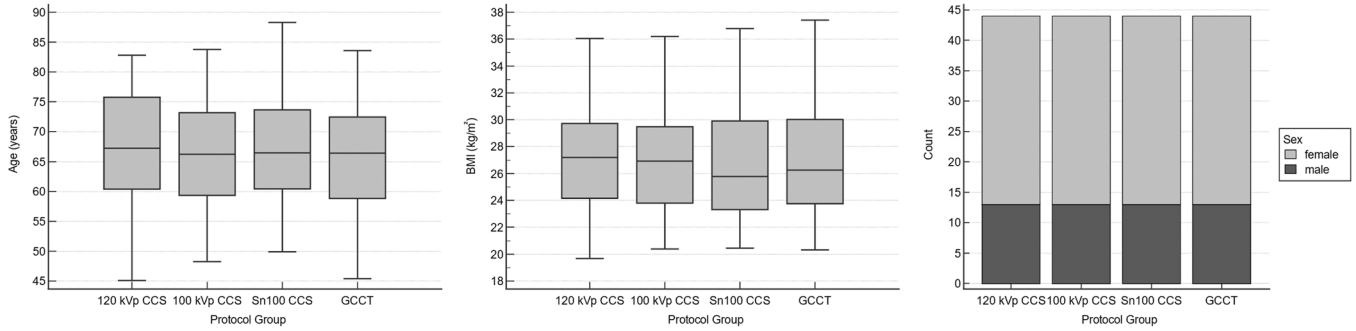

Fig. 1. Demographic parameters of the study population. All subgroups, standard CCS (120 kVp, 100 kVp, Sn100) and GCCT, showed a comparable distribution with regard to age, BMI, and sex (all p = n.s.).

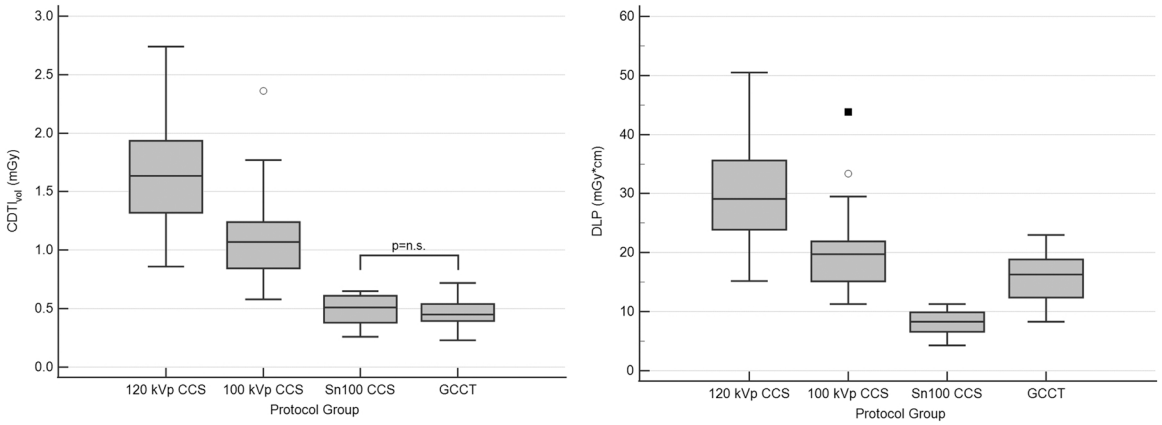

Fig. 2. Radiation exposure of the subgroups. $CTDI_{vol}$ did not differ significantly between Sn100 CCS and GCCT, whereas the DLP of the GCCT scans was significantly higher due to the longer scan length. All other differences were also statistically significant. Of note, the DLP of the GCCT scan was lower than that of standard 120 kVp CCS and 100 kVp CCS.

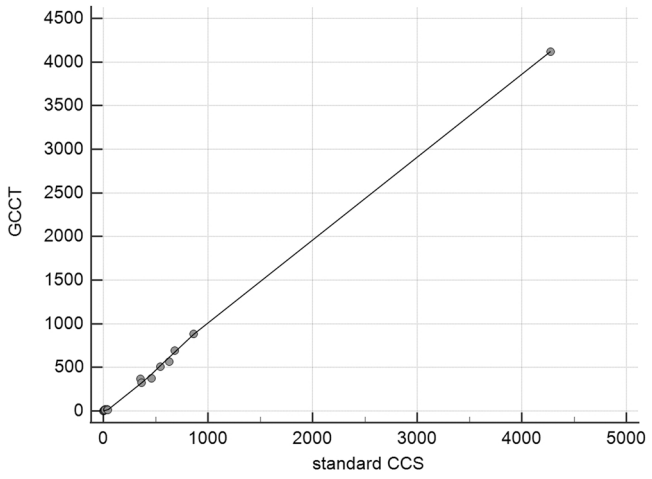

Fig. 3. Correlation of Agatston score equivalents between standard CCS and GCCT scans. The Agatston score equivalent, semi-automatically measured by experts in a subgroup of 20 patients (66.1 (60.7–71.6) years, 6 men, 14 women) who underwent both standard Sn100 CCS and GCCT scans, showed a strong correlation ($\rho = 0.98$, $p < 0.001$). Local regression smoothing trendline with a span of 50%.

radiation exposure in clinical routine. In this study, three dose-saving techniques were combined to enable ECG-gated CACS in chest CT scans with ultra-low dose radiation exposure: high-pitch spiral acquisition, low tube potential, and tin-filtering. While the high-pitch spiral acquisition allows for dose reductions compared to standard or sequential acquisition modes, it also provides a high temporal resolution of 66 ms decreasing the risk of significant motion artifacts. The median acquisition time of the GCCT scan was 0.55 s and, thus, would allow for the examination of poor breath holders, e.g., patients with COPD. Image quality of reconstructions for CACS and for the chest assessment was good, allowing for diagnostic image assessment in all cases of the study population. Patients showed a wide variety of chest pathologies and in nearly one in six patients further diagnostic work-up or follow-up examinations were recommended underlining the clinical purpose of a combined lung and CAD screening approach.

4.3. *Dose savings and diagnostic image quality*

The reduction of the tube potential from 120 kVp to 100 kVp resulted in a decrease in radiation exposure of approximately a third in the CCS, which is in line with a study by Marwan et al. comparing high-pitch CCS with 120 kVp and 100 kVp and a fixed tube current of 80 mAs [29]. The reduction of the tube potential results in a decrease of the average photon energy and, thus, increases the attenuation possibly affecting CACS. However, the addition of a tin-filter reduces the proportion of low-energy photons at a given tube potential and, therefore, increases the average photon energy counteracting the effect of the high attenuation in low-energy parts of the X-ray spectrum. In a phantom study by McQuiston et al. comparing sequential 120 kVp, high-pitch 120 kVp, and high-pitch Sn100 CCS, Agatston scores were not significantly affected when using filtered back projection, whereas the application of iterative reconstruction models resulted in lower Agatston scores in the Sn100 group [30]. The use of the calcium-aware reconstruction kernel Sa36, which was also employed in our study, resulted in comparable

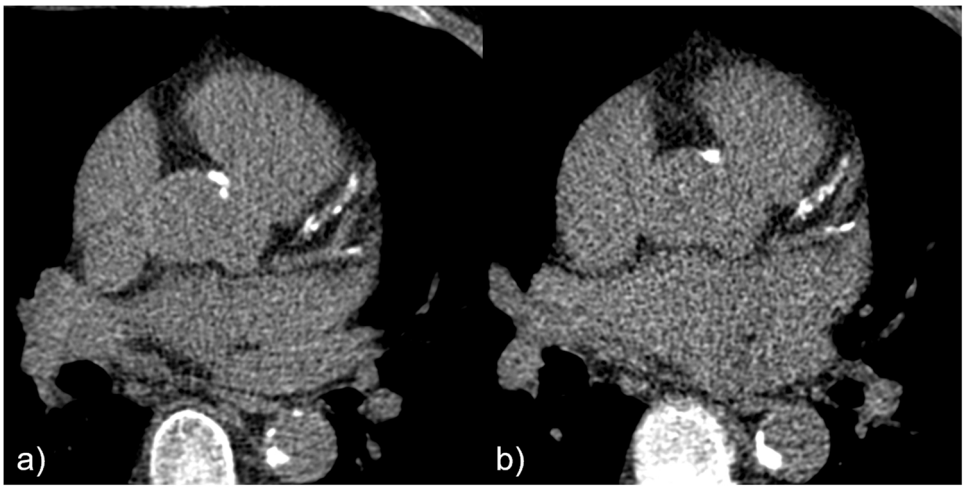

Fig. 4. Example of similar Agatston score equivalents derived from standard CCS and GCCT scans. CACS based on a) standard CCS (Sn100, DLP 8.4 mGy*cm) and b) GCCT scan (DLP 18.0 mGy*cm) resulted in similar Agatston score equivalents (863.0 and 880.6) in a 64-year-old man with normal BMI (22.6 kg/m^2).

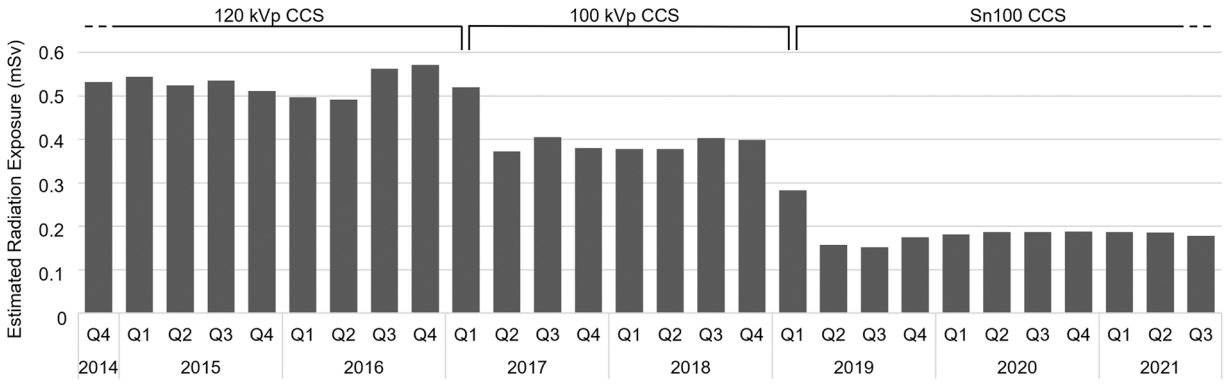

Fig. 5. Estimated radiation exposure from CCS over time. Mean radiation exposure of CCS declined significantly over time due to the increased use of dose-saving techniques as tube potential reduction and tin-filtering (n = 10 481). Q: quarter.

Agatston scores in a wide range of tube voltage settings (70–150 kVp) inclusive of Sn100 in another phantom study [31]. Apfaltrer et al. demonstrated in a clinical study of 78 patients an excellent agreement in Agatston score and percentile-based cardiac risk categorization between Sn100 and 120 kVp high-pitch protocols [32]. In our study, the quantification of the coronary artery calcifications measured by the Agatston score equivalent showed a strong correlation between the GCCT scans and standard CCS in both the semi-automatic as well as AI analyses. Of note, the classification of the coronary artery calcification severity using six different classes showed also an excellent agreement resulting in equal risk stratification. Hence, the GCCT can take advantage of the profound data basis of the well-established Agatston score. Since AI calcification measurements on standard CCS and GCCT scans yielded comparable results, the GCCT is suitable for automatic image processing. This is particularly of interest for high-volume screening approaches such as combined heart and lung assessment in risk populations.

4.4. Clinical relevance of diagnostic radiation exposure

Estimated radiation exposure of the GCCT scans was higher than that of the Sn100 CCS due to the higher scan length. However, radiation exposure of the GCCT scans, which include the entire chest, was lower than of standard 120 kVp or 100 kVp CCS, which assess only the heart and the adjacent lungs. A combined CAD and lung cancer screening can therefore be done with less radiation exposure than these standard CCS by applying the GCCT protocol. $CTDI_{vol}$ values of the GCCT were lower than those recommended for lung cancer screening by the American College of Radiology and the European Society of Thoracic Imaging [33–35]. The median effective radiation dose of the GCCT scans was 0.28 mSv whereas ranges from 0.65 mSv to 2.36 mSv for lung cancer screening were reported in a recent systematic review [36]. The median BMI of the GCCT group was 26.2 kg/m^2, thus reflecting patient characteristics in clinical routine. Although the health impact of low-dose radiation is still a matter of debate, the radiation dose of < 0.5 mSv is well below the average worldwide natural background radiation of 2.4 mSv and risk populations for lung cancer and CAD, e.g., smokers may even have considerably higher radiation exposure [37,38]. Radiation exposure from lung cancer screening CT can be considered acceptable due to the substantial mortality reduction associated with screening [39]. As the GCCT additionally provides a CAD risk assessment at even lower radiation doses, the overall clinical benefits may be even higher. Since this is the first study assessing the GCCT for the simultaneous assessment of heart and lungs, these findings may contribute to the advancement of combined screening approaches in clinical routine.

4.5. Limitations

Accounting for the moderate size of the subgroups, patients of the standard CCS groups were individually matched with regard to age, sex, and BMI to the subjects of the GCCT group resulting in highly comparable distributions. As data analyzed in this study were obtained from a

clinical registry, prospective trials are needed to assess the impact of the GCCT on risk stratification and outcome in risk populations.

5. Conclusions

In conclusion, the novel GCCT allows for a combined CAD and lung cancer screening. Agatston score equivalents showed excellent agreement with standard CCS in both semi-automatic as well as AI analyses, resulting in equivalent risk stratifications. The estimated radiation exposure was well below current values for lung cancer screening and current recommendations, making the GCCT suitable for clinical application, especially in screening programs.

Funding Information

The Radiology Center received a research grant from Siemens Healthcare.

Funding statement

The institution from which the study originated received a research grant from Siemens Healthcare and one of the co-authors is an employee of Siemens Healthcare. The other authors had full control of the data, which were obtained in the study and presented in the manuscript.

CRediT authorship contribution statement

Florian Andre: Conceptualization, Methodology, Formal analysis, Writing – original draft. **Sebastian Seitz:** Data curation, Writing – review & editing. **Philipp Fortner:** Conceptualization, Investigation, Writing – original draft. **Thomas Allmendinger:** Resources, Supervision, Writing – review & editing. **André Sommer:** Investigation, Writing – review & editing, Funding acquisition. **Matthias Brado:** Writing – review & editing. **Roman Sokiranski:** Writing – review & editing. **Joana Fink:** Writing – review & editing. **Hans-Ulrich Kauczor:** Writing – review & editing. **Claus P. Heussel:** Writing – review & editing. **Felix Herth:** Writing – review & editing. **Norbert Frey:** Supervision, Writing – review & editing. **Johannes Görich:** Conceptualization, Investigation, Writing – review & editing, Funding acquisition. **Sebastian J. Buss:** Conceptualization, Methodology, Project administration, Investigation, Writing – original draft.

Conflict of Interest

None of the authors declares a conflict of interests.

Acknowledgements

We thank Ailís Haney for the linguistic revision of the manuscript.

Ethical statement

The study was performed in accordance with the Declaration of Helsinki and was approved be the local ethics committee. The registry study is listed at clinicaltrials.gov (NCT03815123).

References

[1] World Health Organization, The top 10 causes of death, 2020. https://www.who.int/news-room/fact-sheets/detail/the-top-10-causes-of-death. (Accessed July 15th 2021).

[2] H.J. de Koning, C.M. van der Aalst, P.A. de Jong, E.T. Scholten, K. Nackaerts, M. A. Heuvelmans, J.J. Lammers, C. Weenink, U. Yousaf-Khan, N. Horeweg, S. van 't Westeinde, M. Prokop, W.P. Mali, F.A.A. Mohamed Hoesein, P.M.A. van Ooijen, J. Aerts, M.A. den Bakker, E. Thunnissen, J. Verschakelen, R. Vliegenthart, J. E. Walter, K. Ten Haaf, H.J.M. Groen, M. Oudkerk, Reduced Lung-Cancer Mortality with Volume CT Screening in a Randomized Trial, N. Engl. J. Med. 382 (6) (2020) 503–513.

[3] R.L. Siegel, K.D. Miller, A. Jemal, Cancer statistics, 2019, CA Cancer J. Clin. 69 (1) (2019) 7–34.

[4] U.S.P.S.T. Force, A.H. Krist, K.W. Davidson, C.M. Mangione, M.J. Barry, M. Cabana, A.B. Caughey, E.M. Davis, K.E. Donahue, C.A. Doubeni, M. Kubik, C. S. Landefeld, L. Li, G. Ogedegbe, D.K. Owens, L. Pbert, M. Silverstein, J. Stevermer, C.W. Tseng, J.B. Wong, Screening for lung cancer: US preventive services task force recommendation statement, JAMA 325 (10) (2021) 962–970.

[5] H.U. Kauczor, A.M. Baird, T.G. Blum, L. Bonomo, C. Bostantzoglou, O. Burghuber, B. Cepicka, A. Comanescu, S. Couraud, A. Devaraj, V. Jespersen, S. Morozov, I. Nardi Agmon, N. Peled, P. Powell, H. Prosch, S. Ravara, J. Rawlinson, M.P. Revel, M. Silva, A. Snoeckx, B. van Ginneken, J.P. van Meerbeeck, C. Vardavas, O. von Stackelberg, M. Gaga, R. European Society of, S. the European Respiratory, ESR/ERS statement paper on lung cancer screening, Eur. Respir. J. 55 (2) (2020).

[6] M. Ruparel, S.L. Quaife, J.L. Dickson, C. Horst, S. Burke, M. Taylor, A. Ahmed, P. Shaw, M.-J. Soo, A. Nair, A. Devaraj, E.L. O'Dowd, A. Bhowmik, N. Navani, K. Sennett, S.W. Duffy, D.R. Baldwin, R. Sofat, R.S. Patel, A. Hingorani, S.M. Janes, Evaluation of cardiovascular risk in a lung cancer screening cohort, Thorax 74 (12) (2019) 1140–1146.

[7] P.C. Jacobs, M.J. Gondrie, Y. van der Graaf, H.J. de Koning, I. Isgum, B. van Ginneken, W.P. Mali, Coronary artery calcium can predict all-cause mortality and cardiovascular events on low-dose CT screening for lung cancer, Ajr. Am. J. Roentgenol. 198 (3) (2012) 505–511.

[8] J. Shemesh, C.I. Henschke, D. Shaham, R. Yip, A.O. Farooqi, M.D. Cham, D. I. McCauley, M. Chen, J.P. Smith, D.M. Libby, M.W. Pasmantier, D.F. Yankelevitz, Ordinal scoring of coronary artery calcifications on low-dose CT scans of the chest is predictive of death from cardiovascular disease, Radiology 257 (2) (2010) 541–548.

[9] H.S. Hecht, Coronary artery calcium scanning: past, present, and future, JACC Cardiovasc Imaging 8 (5) (2015) 579–596, https://doi.org/10.1016/j.jcmg.2015.02.006.

[10] H. Haubenreisser, M. Meyer, S. Sudarski, T. Allmendinger, S.O. Schoenberg, T. Henzler, Unenhanced third-generation dual-source chest CT using a tin filter for spectral shaping at 100kVp, Eur. J. Radio. 84 (8) (2015) 1608–1613.

[11] M. Vonder, N.R. van der Werf, T. Leiner, M.J.W. Greuter, D. Fleischmann, R. Vliegenthart, M. Oudkerk, M.J. Willemink, The impact of dose reduction on the quantification of coronary artery calcifications and risk categorization: a systematic review, J. Cardiovasc Comput. Tomogr. 12 (5) (2018) 352–363.

[12] M. Vonder, M.D. Dorrius, R. Vliegenthart, Latest CT technologies in lung cancer screening: protocols and radiation dose reduction, Transl. Lung Cancer Res. 10 (2) (2021) 1154–1164.

[13] V. Vingiani, A.F. Abadia, U.J. Schoepf, A.M. Fischer, A. Varga-Szemes, P. Sahbaee, T. Allmendinger, C. Tesche, L.P. Griffith, R. Marano, S.S. Martin, Low-kV coronary artery calcium scoring with tin filtration using a kV-independent reconstruction algorithm, J. Cardiovasc Comput. Tomogr. 14 (3) (2020) 246–250.

[14] D.J. Winkel, V.R. Suryanarayana, A.M. Ali, J. Gorich, S.J. Buss, A. Mendoza, C. Schwemmer, P. Sharma, U.J. Schoepf, S. Rapaka, Deep learning for vessel-specific coronary artery calcium scoring: validation on a multi-centre dataset, Eur Heart J Cardiovasc Imaging (2021), https://doi.org/10.1093/ehjci/jeab119.

[15] P. Perrone-Filardi, S. Achenbach, S. Mohlenkamp, Z. Reiner, G. Sambuceti, J. D. Schuijf, E. Van der Wall, P.A. Kaufmann, J. Knuuti, S. Schroeder, M.J. Zellweger, Cardiac computed tomography and myocardial perfusion scintigraphy for risk stratification in asymptomatic individuals without known cardiovascular disease: a position statement of the Working Group on Nuclear Cardiology and Cardiac CT of the European Society of Cardiology, Eur. Heart J. 32 (16) (2011) 1986–1993, 1993a, 1993b.

[16] J.R. Mayo, J.A. Leipsic, Radiation dose in cardiac CT, Ajr. Am. J. Roentgenol. 192 (3) (2009) 646–653.

[17] H.S. Hecht, C. Henschke, D. Yankelevitz, V. Fuster, J. Narula, Combined detection of coronary artery disease and lung cancer, Eur. Heart J. 35 (40) (2014) 2792–2796.

[18] P. Greenland, M.J. Blaha, M.J. Budoff, R. Erbel, K.E. Watson, Coronary calcium score and cardiovascular risk, J. Am. Coll. Cardiol. 72 (4) (2018) 434–447.

[19] A. Leigh, J.W. McEvoy, P. Garg, J.J. Carr, V. Sandfort, E.C. Oelsner, M. Budoff, D. Herrington, J. Yeboah, Coronary artery calcium scores and atherosclerotic cardiovascular disease risk stratification in smokers, JACC Cardiovasc Imaging 12 (5) (2019) 852–861.

[20] J.R. Watts Jr., S.K. Sonavane, J. Snell-Bergeon, H. Nath, Visual scoring of coronary artery calcification in lung cancer screening computed tomography: association with all-cause and cardiovascular mortality risk, Coron. Artery Dis. 26 (2) (2015) 157–162.

[21] H.S. Hecht, P. Cronin, M.J. Blaha, M.J. Budoff, E.A. Kazerooni, J. Narula, D. Yankelevitz, S. Abbara, 2016 SCCT/STR guidelines for coronary artery calcium scoring of noncontrast noncardiac chest CT scans: a report of the society of cardiovascular computed tomography and society of thoracic radiology, J. Cardiovasc Comput. Tomogr. 11 (1) (2017) 74–84.

[22] O. Dzaye, P. Berning, Z.A. Dardari, M.B. Mortensen, C.H. Marshall, K. Nasir, M. J. Budoff, R.S. Blumenthal, S.P. Whelton, M.J. Blaha, Coronary artery calcium is associated with increased risk for lung and colorectal cancer in men and women: the Multi-Ethnic Study of Atherosclerosis (MESA), Eur. Heart J. Cardiovasc Imaging 23 (5) (2022) 708–716.

[23] X. Xie, Y. Zhao, G.H. de Bock, P.A. de Jong, W.P. Mali, M. Oudkerk, R. Vliegenthart, Validation and prognosis of coronary artery calcium scoring in nontriggered thoracic computed tomography: systematic review and meta-analysis, Circ. Cardiovasc. Imaging 6 (4) (2013) 514–521.

[24] M.T. Wu, P. Yang, Y.L. Huang, J.S. Chen, C.C. Chuo, C. Yeh, R.S. Chang, Coronary arterial calcification on low-dose ungated MDCT for lung cancer screening:

concordance study with dedicated cardiac CT, Ajr. Am. J. Roentgenol. 190 (4) (2008) 923–928.
[25] P.C. Jacobs, I. Isgum, M.J. Gondrie, W.P. Mali, B. van Ginneken, M. Prokop, Y. van der Graaf, Coronary artery calcification scoring in low-dose ungated CT screening for lung cancer: interscan agreement, Ajr. Am. J. Roentgenol. 194 (5) (2010) 1244–1249.
[26] H. Hecht, M.J. Blaha, D.S. Berman, K. Nasir, M. Budoff, J. Leipsic, R. Blankstein, J. Narula, J. Rumberger, L.J. Shaw, Clinical indications for coronary artery calcium scoring in asymptomatic patients: expert consensus statement from the society of cardiovascular computed tomography, J. Cardiovasc Comput. Tomogr. 11 (2) (2017) 157–168.
[27] M.J. Budoff, K. Nasir, G.L. Kinney, J.E. Hokanson, R.G. Barr, R. Steiner, H. Nath, C. Lopez-Garcia, J. Black-Shinn, R. Casaburi, Coronary artery and thoracic calcium on noncontrast thoracic CT scans: comparison of ungated and gated examinations in patients from the COPD Gene cohort, J. Cardiovasc Comput. Tomogr. 5 (2) (2011) 113–118.
[28] L. Azour, M.A. Kadoch, T.J. Ward, C.D. Eber, A.H. Jacobi, Estimation of cardiovascular risk on routine chest CT: ordinal coronary artery calcium scoring as an accurate predictor of Agatston score ranges, J. Cardiovasc Comput. Tomogr. 11 (1) (2017) 8–15.
[29] M. Marwan, C. Mettin, T. Pflederer, M. Seltmann, A. Schuhback, G. Muschiol, D. Ropers, W.G. Daniel, S. Achenbach, Very low-dose coronary artery calcium scanning with high-pitch spiral acquisition mode: comparison between 120-kV and 100-kV tube voltage protocols, J. Cardiovasc Comput. Tomogr. 7 (1) (2013) 32–38.
[30] A.D. McQuiston, G. Muscogiuri, U.J. Schoepf, F.G. Meinel, C. Canstein, A. Varga-Szemes, P.M. Cannao, J.L. Wichmann, T. Allmendinger, R. Vliegenthart, C.N. De, Cecco, Approaches to ultra-low radiation dose coronary artery calcium scoring based on 3rd generation dual-source CT: a phantom study, Eur. J. Radio. 85 (1) (2016) 39–47.
[31] R. Booij, N.R. van der Werf, R.P.J. Budde, D. Bos, M. van Straten, Dose reduction for CT coronary calcium scoring with a calcium-aware image reconstruction technique: a phantom study, Eur. Radio. 30 (6) (2020) 3346–3355.
[32] G. Apfaltrer, M.H. Albrecht, U.J. Schoepf, T.M. Duguay, C.N. De Cecco, J. W. Nance, D. De Santis, P. Apfaltrer, M.H. Eid, C.D. Eason, Z.M. Thompson, M. J. Bauer, A. Varga-Szemes, B.E. Jacobs, E. Sorantin, C. Tesche, High-pitch low-voltage CT coronary artery calcium scoring with tin filtration: accuracy and radiation dose reduction, Eur. Radio. 28 (7) (2018) 3097–3104.
[33] M. Revel, Chest CT for Lung Cancer Screening - Technical standards, European Society of Thoracic Imaging, 2020. https://www.myesti.org/content-esti/uploads/ESTI-LCS-technical-standards_2019-06-14.pdf.
[34] E.A. Kazerooni, J.H. Austin, W.C. Black, D.S. Dyer, T.R. Hazelton, A.N. Leung, M. F. McNitt-Gray, R.F. Munden, S. Pipavath, R. American College of, R. Society of Thoracic, ACR-STR practice parameter for the performance and reporting of lung cancer screening thoracic computed tomography (CT): 2014 (Resolution 4), J. Thorac. Imaging 29 (5) (2014) 310–316.
[35] ACR-STR Practice Parameter for the Performance and Reporting of Lung Cancer Screening Thoracic Computed Tomography (CT) Resolution 4, American College of Radiology, 2019. https://www.acr.org/-/media/ACR/Files/Practice-Parameters/CT-LungCaScr.pdf.
[36] D.E. Jonas, D.S. Reuland, S.M. Reddy, M. Nagle, S.D. Clark, R.P. Weber, C. Enyioha, T.L. Malo, A.T. Brenner, C. Armstrong, M. Coker-Schwimmer, J. C. Middleton, C. Voisin, R.P. Harris, Screening for lung cancer with low-dose computed tomography: updated evidence report and systematic review for the us preventive services task force, JAMA 325 (10) (2021) 971–987.
[37] Radiation: effects and sources, United Nations Environment Programme, 2016.
[38] A. Vaiserman, A. Koliada, O. Zabuga, Y. Socol, Health impacts of low-dose ionizing radiation: current scientific debates and regulatory issues, Dose Response 16 (3) (2018), 1559325818796331.
[39] C. Rampinelli, P. De Marco, D. Origgi, P. Maisonneuve, M. Casiraghi, G. Veronesi, L. Spaggiari, M. Bellomi, Exposure to low dose computed tomography for lung cancer screening and risk of cancer: secondary analysis of trial data and risk-benefit analysis, BMJ 356 (2017) j347.